A. ILJIN,[1,2] D. WEI,[2,3] U. BORTOLOZZO,[2] S. RESIDORI[2]

[1] Institute of Physics, Nat. Acad. of Sci. of Ukraine
(46, Prosp. Nauky, Kyiv 03039, Ukraine; e-mail: lgtc@iop.kiev.ua)
[2] Institute de Physique de Nice, UMR 7010, Université de Nice-Sophia Antipolis, CNRS
(1361, Route des Lucioles, 06560 Valbonne, France)
[3] Beijing Genomics Institute
(Shenzhen, China)

DYNAMIC GRATING RECORDING BY A LIGHT-INDUCED MODIFICATION OF THE ORDER PARAMETER IN DYE-DOPED CHIRAL NEMATIC LIQUID CRYSTALS

UDC 539

The dynamic grating recording in dye-doped chiral nematic liquid crystals is studied. It is shown that the mechanism responsible for the grating recording can be ascribed to a photo-induced modification of the order parameter of a liquid crystal within the range of optical intensities, for which the orientational nonlinearity remains quenched by the structural order of the chiral structure. The two-wave mixing dynamic behavior is analyzed for different intensities of the recording beams, by comparing the self-diffraction regime with the probe diffraction. This allows us to distinguish a particular mechanism of optical nonlinearity. The photo-induced modulation of the order parameter and the respective changes of medium's refractive indices determine the relatively fast response times, local nonlinear response, and quite high diffraction efficiency within an extremely wide intensity range (more than three orders of magnitude) The chiral helical structure hinders the nematic director reorientation, prevents the appearance of surface effects, and is very favorable for the nonlinear control over a polarization. Such new mechanism could also be extended to the recording of arbitrary phase profiles as requested in several applications for the manipulation of a light beam.

K e y w o r d s: nonlinear optics, two-wave mixing, dynamic gratings, liquid crystals, cholesterics, light-induced order modification.

1. Introduction

During last decades, liquid crystalline (LC) compounds have been proved extremely promising media that exhibit a vast majority of nonlinear optical effects being essentially enhanced for dye-doped mixtures, in which the dye molecules stimulate a reorientation of the LC director [1]. This collective behavior of molecules in a bulk LC under the action of light takes place either because of surface effects [2, 3] or due to the recurring *trans*-to-*cis* conformational changes of a dye [4]. Owing to the elastic forces, the LC director reorientation spreads, however, outside the illuminated region making the nonlinear optical response substantially nonlocal.

Chiral nematic liquid crystals (CLCs) characterized by a self-assembled helical structure of their molecular arrangement represent a natural photonic crystal and show unique optical properties such as the selective Bragg reflection for circularly polarized

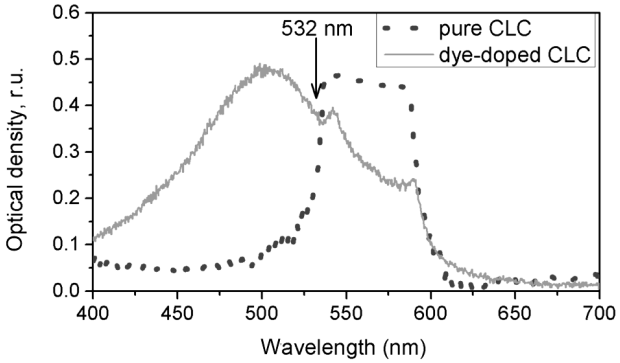

Fig. 1. Optical density spectra of SR band of pure CLC mixture and MR absorption in dye-doped chiral liquid crystals

light [5]. The easiness to change the pitch with external fields, with temperature [6], or light [7] makes the dye-doped CLCs highly attractive for applications such as tuneable lasers [8] or photo switchable bandgaps, as recently been demonstrated for photosensitized CLCs [9, 10].

Previous experiments in dye-doped CLCs have shown that an undisturbed helix regime occurs at low pump intensities, which is characterized with a relatively fast response time, high gain and spatial resolution [11], the modulation of the cell transmittance, and subsequent two-beam coupling effects [12]. In addition, slow and stored light applications have been demonstrated with this type of media [12]. Indeed, at low light intensities, the helical structure inhibits the molecular reorientation, while the illumination with light in the absorption band of dopants induces the *tran-cis* transformation of the dyes. At high intensities, the molecular reorientation occurs, by provoking a helix perturbation. Here, we show that, up to the regimes of light-induced helix destruction, the increasing population of *cis* isomers and the consequent photo-induced modification of the order parameter of LC results in a change in the CLC refractive indices. In the current experiments, the light-induced order parameter modification (LIOM) is revealed by the appearance of several diffraction orders before the unwinding of the helix takes place and dominates the process leading to the light scattering in multiple directions. The LIOM-model allowed a quantitative evaluation of the processes of diffraction grating recording and appears to be in agreement with the experimental data over the broad range of the pumping light intensities.

2. Methods/Experimental

Materials and samples

The employed LC-cells have comprised glass plates, the gap between which was set with uniform calibrated spacers 25÷30 μm in thickness. The inner surfaces of the substrates were covered with either rubbed PVA (polyvinyl-alcohol) or with another orienting polymer [13] that encourages the planar anchoring. Particular techniques of surface treatment and cell fabrication could be found elsewhere [14]. The cells were filled with a chiral nematic liquid crystal (a mixture of E7 nematic host with 40 wt.% of CB15 chiral dopant) with dissolved ∼0.3 wt.% of the Methyl-Red (MR) dye (sodium salt). The spectra of the optical density of cells containing the pure CLC compound (revealing the selective reflection band) and the dye-doped chiral liquid crystal mixture are presented in Fig. 1.

2.1. Experimental set-up

Dye-doped CLC cells were investigated by means of the two-wave mixing technique (TWM), which is widely applied to the investigations of nonlinear optical properties of optical Kerr-like media [15]. A fringe pattern appearing due to the interference of two coherent laser beams causes a periodic modulation of medium's refractive index in the illuminated area, i.e., a phase diffraction grating is formed. The grating could be considered thin under current experimental conditions as the Klein parameter [16] appears to be much less of the unity: $Q = \frac{2\pi\lambda d}{\bar{n}\Lambda^2} \approx 0.15$ ($\lambda$is the light wavelength, d is the grating thickness, Λ is the grating period, and $\bar{n}$ is the average refractive index). When a light wave passes through such a grating, many diffraction orders will appear in the output (the so-called Raman–Nath regime) with the intensity of the n-th order being determined by $I_n = \eta_n I_0$ (I_n and I_0 are the intensities of the diffracting and input beams, respectively, η_n is the efficiency of diffraction into the n-th order) [17].

Dynamic diffraction gratings were induced in the ordinary two-beam-coupling arrangement (Fig. 2) by means of the second harmonic of the continuous-wave YAG laser (radiation wavelength 532 nm, the total output power was tuned within the range 48 μW÷70 mW, the illuminated spot diameter was ∼3 mm). The variation of the angle between the writing beams, θ, allowed the adjustment of the period of

the interference pattern, and, hence, of the grating period, Λ, within the interval 13–55 μm. The detection of the grating has been performed by monitoring the higher diffraction orders in the self-diffraction regime or via the diffraction of the probe beam from a He–Ne laser (with a wavelength of 633 nm and the power ∼1 mW). Temporal changes of the power of the first orders of diffraction of the both pumping and probing beams were measured with photodiodes (ThorLabs) and recorded with the help of a two-channel digital oscilloscope Tectronix TDS-220. No special temperature stabilization of the cell has been used in the experiments; however, the laboratory room climatic system kept the environment temperature at 20 °C.

3. Results and Discussions

3.1. Nonlinear recording of dynamic diffraction gratings

Typical oscilloscope traces of the two signals are presented in Fig. 3. At the opening of the pumping beams ($t = 0$), an efficient intensity growth has been observed for both the diffracting probe and self-diffracting beams. The qualitative comparison between the two curves shows that both the writing and probe beams undergo a similar behavior with the signal passing through a maximum and, then, approaching the saturation at some intermediate value.

After the pumping beams are cut off, the grating decay can be analyzed by observing the relaxation dynamics of the probe beam. The changes of the diffracted probe depend on the pumping intensity – the higher the intensity, the faster the maximum is reached. The noticeable probe diffraction is already observed at very low pumping intensities – of the order of 1 mW/cm^2 (Fig. 4, *a*). Then the grating efficiency grows greater with the pumping intensity, and more diffracted orders are observed both in the self-diffracted beam and in the probe diffraction (Fig. 4, *b* and *c*). The process continues until the texture transition of CLC occurs and causes an extreme scattering (Fig. 4, *d*). This "overdrive" regime appears at intensities by 3 orders of magnitude greater (∼1 W/cm^2) than that of the first grating observations. At these values of the pumping intensities, the character of the light scattering changes drastically, and this transition reveals a complex modulation of the LC director distribution due to transverse helix undulations (Fig. 4, *d*).

The used CLC mixture reveals the temperature stability of its helical pitch [18, 19], i.e., it is possible to rule out the influence of the heating on the LC director winding and, thus, on the modulation of the refractive indices due to a shift of the photonic

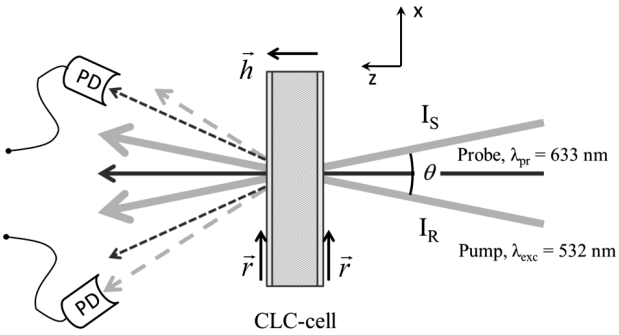

Fig. 2. Experimental arrangement of two-wave mixing experiments in the dye-doped CLC cell; PD: photodiode, *h*: helical axis, *r*: rubbing direction

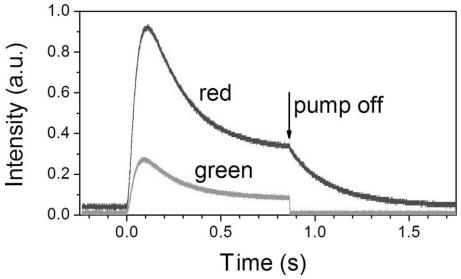

Fig. 3. Typical oscilloscope traces of the 1st diffracting orders of probe (red) and pump beams (green), $t = 0$ is "pump on"

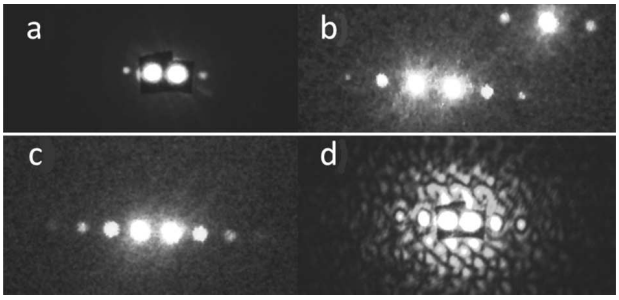

Fig. 4. Light scattering at different pump intensities. Self-diffraction of the pump beam for I = 3 mW/cm^2 (*a*), I = = 15 mW/cm^2 (*b*), I = 75 mW/cm^2 (*c*), I = 1 W/cm^2 (*d*). Diffraction of the probe He–Ne-laser beam is presented for illustration in the inset in panel (*b*)

band gap, since the position of the selective reflection band remains stable at the green light illumination up to intensities about 180 mW/cm^2 [20]. Moreover, the heating itself could not cause an enough refractive index modulation, as the temperature increase was estimated on the order of fractions of K.

3.2. Light-induced modification of the LC order parameter

The mechanism of LC director reorientation, i.e., orientational nonlinearity, is generally invoked in the description of light-induced optical changes in an MR-doped nematic LC (see, e.g., Ref. [1] for a review). While the presence of this mechanism claims no doubts for the experiments with dye-doped nematic LCs and in cells with a long-pitch chiral nematic LC [21], it could hardly be employed in the current case with comparatively short-pitch CLC and low pumping intensities. Indeed, due to the severe steepness of the Freedericksz transition with respect to the applied field strength, the out-of-plane deviation of the LC director results very soon in the unwinding of the chiral helix and leads to the texture breaking with a further increase in the intensity. More precisely, because of the intrinsic helical winding of CLC, even a minor director reorientation out of a quasinematic plane causes the appearance of periodic undulations of the CLC planar texture, as first reported in [22]. In the experiments described here, however, the CLC Grandjean texture remains undisturbed within a very large intensity range and becomes unstable only under the illumination with very strong intensity (Fig. 4, *d*), producing periodic structures similar to those reported in [22].

The description of light-induced changes of the optical properties of the CLC medium can be accounted for by starting to consider the effects imposed by the light absorption upon the dye molecules. Let us consider a photo-excitable system with exactly two optically active states corresponding to the *trans-* and *cis*-conformational states of dye molecules. The illumination of such a system with light of intensity I and with wavelength λ falling inside the dye absorption band will result in an increase in the population of the *cis* state and, correspondingly, in the depopulation of the *trans* state [23].

In the general case, the concentration of the photo-transformed molecules, $c_{\rm ph}$, can be described by the kinetic equation

$$\frac{dc_{\rm ph}}{dt} = \alpha_T\left(1 - c_{\rm ph}\right) I - \alpha_C c_{\rm ph} I - \Gamma c_{\rm ph} + D_{\rm eff}\nabla^2 c_{\rm ph}. \tag{1}$$

Here, α_T, α_C represent the efficiency of light-stimulated *trans-cis* and *cis-trans* photo-isomerizations. Correspondingly, the last two terms refer to the spontaneous reverse thermal *cis-trans* transition and molecular diffusion, respectively, where Γ is the thermal coefficient, and $D_{\rm eff}$ is the diffusion coefficient of the photo-transformed molecules.

During the light-induced transformation of molecules as, for instance, in the process of *trans-cis* photo-isomerization, the concentration of photo-transformed molecules (i.e., MR *cis*-isomers) depends on the exposure time and pumping light intensity: $c_{\rm ph}(t) = c_\infty - (c_\infty - c_0)\exp(-t/\tau_{\rm ph})$, where the characteristic time of the process is $\tau_{\rm ph} = (\alpha_T + \alpha_C)^{-1} I^{-1}$, and c_0 and c_∞ are the initial and final, saturated, dye concentrations in the *cis*-form. Correspondingly, the reverse *cis-trans* transition, as well as the isomer diffusion, can be neglected for the moment.

At the intersection of two coherent light beams (S and R stand for the signal and reference beams, respectively), an interference fringe pattern distribution of the light intensity is created, which can be described in one-dimension as $I(x) = I_S + I_R + 2\sqrt{I_S I_R}\cos(qx)$, where x is the coordinate along the transverse beam direction, $q = 2\pi/\Lambda$ the grating wave vector, $\Lambda = \lambda/2\sin(\theta/2)$, with θ being the angle between the two interfering beams, and I_S and I_R are the intensities of the signal beam and, respectively, the reference one.

In the case of equal intensities of the writing beams, $I_S = I_R = I_0$, the resulting modulation of the concentration of light-transformed molecules depends on the recording time as

$$\Delta c_{\rm ph}(x,t) \sim \exp\left(-2\left(1 + \cos(qx)\right) t/\tau_{\rm ph}\right). \tag{2}$$

Note that the recorded grating appeared to be essentially non-sinusoidal at high intensities. The detailed examination of such a phenomenon was previously done in the case of photorefractive crystals [24] and for bacteriorhodopsin [25]. Investigations of the absorption changes accompanying the light-induced *trans-cis* isomerization have shown a variation in the optical density [26]. Studies with the flash pho-

tolysis technique of MR-solutions [27], however, revealed very little changes of the dye absorption after the strong excitation at different light wavelengths (<1%). So, the contribution to the diffraction from the amplitude grating could possibly be safely neglected.

When the concentration of dye molecules is small ($c_{\rm dye} \ll 1$), the modulation of the local refractive indices of a dye-doped liquid crystal could be considered, in the frame of the LIOM-model (Light-Induced Order Modification [18,19]), as being proportional to the concentration of photo-excited dye molecules: $\delta n_{O,E} = -g\alpha_V c_{\rm ph}\Delta n_0$, where the subscripts indicate the ordinary and extraordinary ($g = -1/3$ and $g = 2/3$, respectively) refractive indices, Δn_0 is the initial local birefringence of the CLC medium, and α_V stands for the efficiency of the photo-transformation process.

It is, then, possible to look for the refractive index modulation,$\delta n\,(x,t)$, in the form of a Fourier expansion. Since the grating function is periodic and even, the expansion reduces to

$$\delta n\,(x,t) = \sum_{m=1} n_m\,(t)\cos\,(mqx), \tag{3}$$

where

$$n_m\,(t) = \frac{1}{\pi}\int\limits_{-\Lambda/2}^{\Lambda/2} \delta n\,(x,t)\cos\,(mqx)\,dx.$$

The resulting grating, thus, is composed of a set of harmonic gratings with the amplitudes n_m and the wave vectors mq ($m = 1,2,3,...$). Taking Eq. (2) into account, one can obtain the magnitude of the resulting refractive index modulation for each harmonics:

$$\delta n_m\,(\tilde{\tau}) = \frac{\alpha_V\Delta n_0}{6\pi}\int\limits_{-\Lambda/2}^{\Lambda/2}\cos\,(mqx)\times$$
$$\times\,\exp\,(-2\tilde{\tau}\,(1+\cos\,(mqx)))\,dx. \tag{4}$$

This gives, in the thin-grating approximation, the efficiency of diffraction into the μ-th diffraction order from the m-th grating as: $\eta_\mu^m = J_\mu^2\,(k_\omega\delta n_m d)$, where $k_\omega = 2\pi/\lambda$ is the light wave vector, d is the grating thickness, J_n is the n-th-order Bessel function of the first kind.

The numerical evaluation of integral (4) with the variable parameter $\tilde{\tau} \equiv t/\tau_{\rm ph}$ allows the fitting of the temporal dependences of the first diffracting orders obtained at different pump intensities. Results of the fitting procedure applied to the probe beam diffraction are presented in Fig. 5.

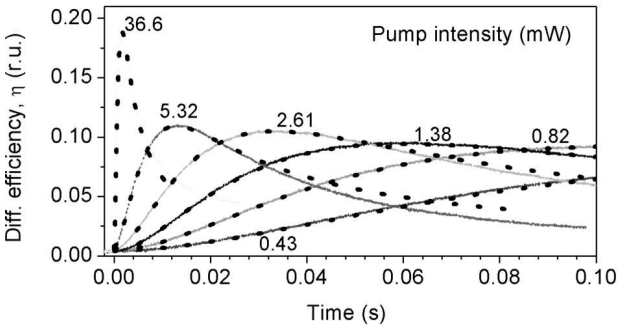

Fig. 5. Oscilloscope traces (solid curves) of the first order test beam diffraction in dependence on the pump light intensity (curve designations in mW) and fitting results (dots)

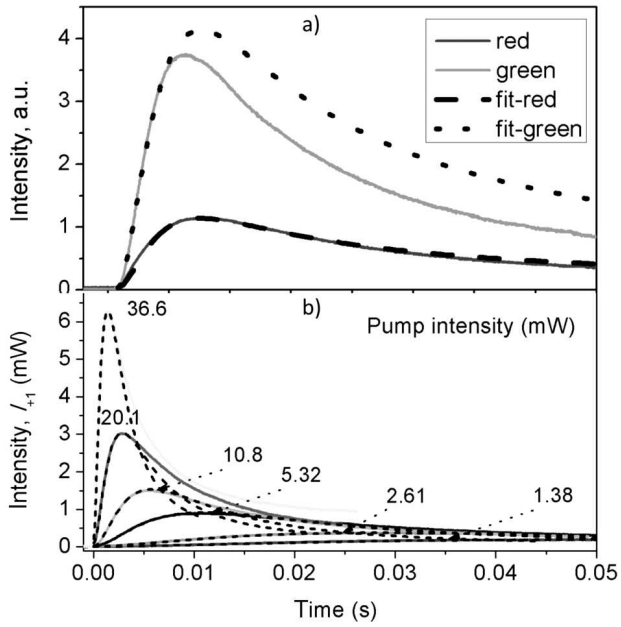

Fig. 6. Fitting mismatch of the self-diffracting beam with η_1^1 (*a*). Results of the fitting (dots) of the first order self-diffraction (solid curves) in dependence on the pump light intensity (curve designations in mW), with the account of the contribution of the second-harmonic grating, η_1^2, and characteristic times $\{\tilde{\tau}_{\rm int}\}$ (*b*)

By this procedure, a set of characteristic times, $\{\tilde{\tau}_{\rm int}\}$, corresponding to the set of pumping light intensities used in the experiment, $\{I_0\}$, has been deter-

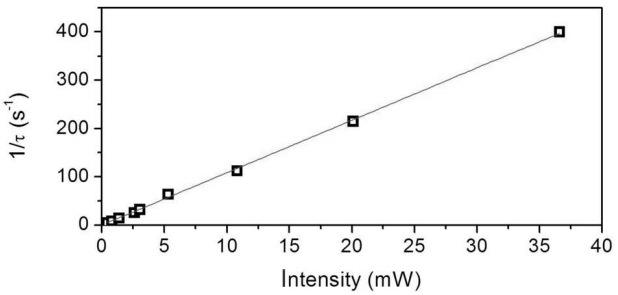

Fig. 7. Dependence of the inverse characteristic time on the pump intensity: squares – experiment, solid line – linear fit

mined. This set of characteristic times ($\{\tilde{\tau}_{\text{int}}\}$) is then used to fit the first-order self-diffraction signal by a variation of the intensity parameter, A, (Fig. 6, *a*). In this case, however, the fit doesn't match well, and an additional input from the second beam is to be taken into account. In conventional photorefractive media, this may concern the second-order diffraction, η_2. In the current case, however, the second-order diffracting wave is to be neglected, while the contribution of the second-harmonic grating, η_1^2, could be quite appreciable. Thus, in Fig. 6, *b*, the corresponding results of the fitting of a signal with $I_{\text{fit}} = A\left(\eta_1^1 - \eta_1^2\right)$ are presented.

3.3. Intensity dependence of characteristic time

The dependence of the inverse characteristic time on the pumping intensity is linear (Fig. 7), which supports the suggested mechanism of photo-induced transformation of MR molecules.

Note that the characteristic times of the molecular diffusion could be estimated of the order of 0.4 s from the typical value of the diffusion coefficient $D = 2 \times \times 10^{-7}$ cm^{2}s^{-1} [27]. With the reciprocal spontaneous *cis-trans* transition time being ∼0.7 s [27], the model derived here for the grating description looks quite appropriate.

4. Conclusions

In conclusion, chiral nematic liquid crystals containing a small amount of MR dye are shown to be an efficient nonlinear medium with large dynamic range and texture stability (light intensities spanned over more than three orders of magnitude). The dynamic gratings have been completely reversible and, unlike the experiments with the MR-doped nematics [28], we have not observed the recording of permanent gratings, at least for the studied CLC mixture and under the employed experimental conditions. The light-induced *trans-cis* isomerization of MR molecules and the subsequent distortion of the LC ordering in the vicinity of a dye molecule (LIOM-mechanism) are used to explain the observed optical nonlinearity, providing relatively fast recording times (∼1 ms and less) and with prospects for the essential future improvement. Being strictly local, the LIOM mechanism allows the high spatial resolution and, hence, the opening of new possibilities for the volume grating recording.

A. Iljin acknowledges financial support from National Academy of Sciences of Ukraine (Program B/197) and the CNRS (exchange visit contract).

1. I.C. Khoo. Nonlinear optics of liquid crystalline materials. *Phys. Rep.* **471**, 221 (2009).
2. F. Simoni, L. Lucchetti, D.E. Lucchetta, O. Francescangeli. On the origin of the huge nonlinear response of dye-doped liquid crystals. *Opt. Express* **9**, 85 (2001).
3. A. Petrossian, S. Residori. Surfactant enhanced reorientation in dye-doped nematic liquid crystals, *Europ. Lett.* **60**, 79 (2002).
4. A. Petrossian, S. Residori. Light driven motion of the nematic director in azo-dye doped liquid crystals, *Opt. Commun.* **228**, 145 (2003).
5. P.G. de Gennes, J. Prost. *The Physics of Liquid Crystals* (Clarendon Press, 1993) [ISBN: 0198520247].
6. G. Chilaya. Cholesteric liquid crystals: optics, electro-optics, and photo-optics, in *Chirality in Liquid Crystals*, edited by H.S. Kitzerow, C. Bahr (Springer, 2001) [ISBN 978-0-387-21642-3].
7. V. Boychuk, I. Gerus, A. Iljin, J. Parka. Light-controlled helical pitch and dynamic gratings. *Opto-Electron. Rev.* **17**, 287 (2009).
8. H. Coles, S. Morris. Liquid-crystal lasers. *Nat. Photonics* **4**, 676 (2010).
9. U.A. Hrozhyk, S.V. Serak, N.V. Tabiryan, T.J. White, T.J. Bunning. Optically switchable, rapidly relaxing cholesteric liquid crystal reflectors. *Opt. Express* **18**, 9651 (2010).
10. U.A. Hrozhyk, S.V. Serak, N.V. Tabiryan, T.J. White, T.J. Bunning. Nonlinear optical properties of fast, photo-switchable cholesteric liquid crystal bandgaps. *Opt. Mater. Express* **1**, 943 (2011).
11. D. Wei, A. Iljin, Z. Cai, S. Residori, U. Bortolozzo. Two-wave mixing in chiral dye-doped nematic liquid crystals. *Opt. Lett.* **37**, 734 (2012).
12. D. Wei, U. Bortolozzo, J.P. Huignard, S. Residori. Slow and stored light by photo-isomerization induced transparency

in dye doped chiral nematics. *Opt. Express* **21**, 19544 (2012).
13. N. Aryasova, A. Iljin, V. Reshetnyak, Yu. Reznikov, A. Gluschenko, J. West. Orientation of nematic liquid crystals on random anchoring surface. *Mol. Cryst. Liq. Cryst.* **375**, 165 (2002).
14. A. Iljin, V. Reshetnyak, S. Shelestiuk, V. Yarmolenko. Surface director sliding in LC cell with light-controlled chirality. *Mol. Cryst. Liq. Cryst.* **453**, 263 (2006).
15. *Photorefractive Materials and Their Applications.* Edited by P. Gunter, J.P. Huignard (Springer, 2006), Vol. 1 [ISBN: 0-387-25191-X].
16. W.R. Klein, B.D. Cook. Unified approach to ultrasonic light diffraction. *IEEE Trans. on Sonics & Ultrasonics* **SU-14**, 123 (1967).
17. S. Residori, U. Bortolozzo, J.P. Huignard. Slow light using wave mixing in liquid crystal light valve. *Appl. Phys. B* **95**, 551 (2009).
18. A. Iljin. Transient modulation of order parameter and optical non-linearity in a chiral nematic liquid crystal. *Mol. Cryst. Liq. Cryst.* **543**, 143 (2011).
19. A. Iljin. Light-induced order modification – the way to speed up. *J. Mol. Liq.* **267**, 28 (2018).
20. D. Wei, S. Residori, U. Bortolozzo. Phase conjugation and slow light in dye-doped chiral nematics. *Opt. Lett.* **37**, 4684 (2012).
21. Y.-J. Wang, M. Pei, P. Peng, G.O. Carlisle. All-optical polarization-independent diffraction in dye-doped cholesteric liquid crystal. *J. Mat. Sci. – Mater. Electronics* **17**, 385 (2006).
22. C.J. Gerritsma, P. Van Zanten. Periodic perturbations in the cholesteric plane texture. *Phys. Lett. A* **37**, 47 (1971).
23. I. Jánossy, L. Szabados. Photoisomerization of azo-dyes in nematic liquid crystals. *J. Nonlin. Opt. Phys. Mater.* **7**, 539 (1998).
24. M. Fally, M. Imlau, R.A. Rupp *et al.* Specific recording kinetics as a general property of unconventional photorefractive media. *Phys. Rev. Lett.* **93**, 243903 (2004).
25. E. Korchemskaya, N. Burykin, S. Bugaychuk *et al.* Dynamic holography in bacteriorhodopsin/gelatinfilms: effects of light–dark adaptation at different humidity. *Photochem. Photobiol.* **83**, 403 (2007).
26. S. Mukherjee, S.C. Bera. Low temperature laser flash photolysis and spectral studies of methyl red. *J. Chem. Soc. Faraday Trans.* **94**, 67 (1998).
27. M. Hara, S. Ichikawa, H. Takezoe, A. Fukuda. Binary mass diffusion constants in nematic liquid crystals studied by forced Rayleigh scattering. *Jpn. J. Appl. Phys.* **23**, 1420 (1984).
28. E. Ouskova, Yu. Reznikov, S.V. Shiyanovskii *et al.* Photoorientation of liquid crystals due to light-induced desorption and adsorption of dye molecules on an aligning surface. *Phys. Rev. E* **64**, 051709 (2001).

Received 05.02.19

А. Ільїн, Д. Вей, У. Бортолоццо, С. Резідорі

ЗАПИС ДИНАМІЧНИХ ҐРАТОК ЗА РАХУНОК ЗМІНИ ПАРАМЕТРА ПОРЯДКУ СВІТЛОМ У КІРАЛЬНИХ НЕМАТИЧНИХ РІДКИХ КРИСТАЛАХ З ДОМІШКОЮ БАРВНИКА

Р е з ю м е

Досліджується запис динамічних ґраток у кіральних нематичних рідких кристалах з домішкою барвника. Показано, що в інтервалі інтенсивностей світла, для якого орієнтаційна нелінійність залишається пригніченою структурним упорядкуванням кіральної структури, механізмом запису може бути фотоіндукована зміна параметра порядку. Аналізується динамічна поведінка змішування двох хвиль для різних інтенсивностей записуючих пучків шляхом порівняння самодифракції з дифракцією зондуючого пучка, що дозволило виділити особливий механізм оптичної нелінійності. Фотоіндукована зміна параметра порядку і відповідні зміни показників заломлення середовища визначають відносно швидкі часи відгуку, локальний нелінійний відгук і вельми значну ефективність дифракції в надзвичайно широкому діапазоні інтенсивностей (більше 3 порядків). Кіральна гелікоідальна структура перешкоджає реорієнтації директора нематика і появі поверхневих ефектів і сприяє нелінійному контролю над поляризацією. Цей новий механізм може бути використаний для запису довільних профілів фази у пристроях для керування пучком світла.